Manual Guidance of Humanoid Robots without Force Sensors: Preliminary Experiments with NAO

Marco Bellaccini   Leonardo Lanari   Antonio Paolillo   Marilena Vendittelli

Abstract— In this paper we propose a method to perform manual guidance with humanoid robots. Manual guidance is a general model of physical interaction: here we focus on guiding a humanoid by its hands. The proposed technique can be, however, used also for joint object transportation and other tasks implying human-humanoid physical interaction. Using a measure of the Instantaneous Capture Point, we develop an equilibrium-based interaction technique that does not require force/torque or vision sensors. It is, therefore, particularly suitable for low-cost humanoids and toys. The proposed method has been experimentally validated on the small humanoid NAO.

I. INTRODUCTION

Physical Human-Robot interaction (pHRi) is attracting an increasing interest in robotics research with a consequent fast progress in both methodological and technological aspects. Most of the results, however, deal with robotic manipulators and their application to humanoids is either not direct or poorly effective because they do not exploit the specificities of these robots related to their mobility system. In addition, for cost reasons, most humanoids are not equipped with the sensors commonly used in physical interaction, like, e.g., force sensors.

In this work we propose a technique for guiding humanoids toward desired walking directions with a specified speed via physical interaction. The distinctive feature of the proposed method resides in the absence of any requirement to use force/torque sensors to measure the interaction forces. The considered physical interaction, herein referred to as manual guidance, includes both simple hand-in-hand guidance (see Fig. 1) and joint object transportation. Here we focus on hand-in-hand guidance.

One of the first examples of this kind of physical interaction is represented by [1] in which the hand-in-hand guidance of the WABIAN humanoid is obtained by monitoring the robot hand position. An impedance controller for joint object transportation with an HRP-2 robot is presented in [2]. A similar method, extended with an appropriate footstep planner, has been proposed and validated on the same robot in [3], while a strategy based on impedance control and a Finite State Machine was proposed in [4] and experimented on a HRP-2 robot.

In the above cited methods the direction of motion is controlled using either the position of the hand (as in [1]), and thus limiting the application of the method to physical

Fig. 1.   Hand-in-hand manual guidance of NAO.

interaction through the hands, or the measurements from the force sensors on the wrists. The standard equipment of humanoids, however, rarely include the presence of force sensors at the wrists to limit the complexity and the cost of the platform. Developing minimal sensing approaches to physical interaction would at the same time overcome this problem and lay the basis for the exploration of new methodologies for pHRi especially suited to humanoid robots. The same minimal sensing spirit is behind the interaction behavior obtained with the Acroban robot in [5] which, however, relies on the dynamic peculiarities of that specific robot.

In this paper we introduce a new equilibrium-based technique that uses the perceived perturbation of the Instantaneous Capture Point (ICP) as a measure of the effect that the interaction force produces on the robot equilibrium. The concept of capture point was introduced in [6] for push recovery and subsequently shown to be effective also for walking control [7], [8], [9].

The interaction technique proposed here is based on the simple observation that when manually guiding a humanoid, the human is supposed to push or pull it toward some intended direction of motion. This interaction force acts as a disturbance on the humanoid Center of Mass (CoM). In particular, the position of the ICP, which depends on CoM position and velocity, moves in the same direction of the force applied by the human. The desired manual guidance is obtained by commanding the robot to walk toward the ICP to maintain the desired equilibrium.

With the proposed method the interaction is not limited to contacts with hands but the application of a force on

any part of the humanoid body producing a perturbation on the ICP can be used to guide the robot walking. The CoM position and velocity are determined using the onboard Inertial Measurement Unit (IMU), always included in the standard sensory equipment, and modeling the robot as a 3D-LIP. To isolate the contribution of the interaction force to the ICP motion, it is necessary to filter out the oscillation due to the walking gait from the CoM position and velocity signals. This oscillation, also known as sway motion, represents a known quasi-periodic disturbance and is filtered through low-pass filters.

The proposed technique has been validated on the small humanoid NAO. Due to the lack of force/torque sensors (except for those under the feet, not used in our approach), NAO is a good platform to show how minimal are the requirements of our method. To keep the method as general as possible, the desired walking velocity is commanded to NAO through its high level locomotion API: any humanoid platform on which similar high-level commands could be executed will be immediately able to perform manual guidance using the proposed approach.

The paper is organized as follows: Section II illustrates the interaction model on which the proposed method relies. Section III presents the concepts behind our walking controller and its practical implementation. Experimental results obtained by applying a constant force to the humanoid NAO and by pulling and pushing it through its hands are presented in Section IV. Finally Section V concludes the paper and draws the lines of future research paths.

II. INTERACTION MODEL

The scenario considered in this paper is depicted in Fig. 1 showing a human guiding the robot NAO by pushing or pulling it through its hands. To simplify the analysis we model the position controlled humanoid NAO as a 3D-LIP with actuated ankle as shown in Fig. 2.

The mass m of the pendulum moves under the action of the torques τ_x, τ_y applied at the pivot joint and the gravity. The mass is assumed to move on a plane at an height held constant by the prismatic joint on the pendulum axis. The position of the CoM is expressed by the vector $(x_c,\ y_c,\ z_c)^T$, with z_c a constant. The force due to the interaction is modeled as an external force $\boldsymbol{f}$ acting on the mass m.

The CoM dynamics of the 3D-LIP in the x and y component are decoupled and can be described by the same formal equation. Therefore, there is no loss of completeness in analyzing only the dynamics in the x component of the motion which can be written as

$$\ddot{x}_c = \omega^2 x_c + \frac{1}{mz_c}\tau_y + \frac{f_x}{m}, \qquad (1)$$

where $\omega = \sqrt{g/z_c}$, g is the gravitational acceleration and f_x is the x component of the external force.

Given the dynamics of the 3D-LIP in eq. (1), the Zero Moment Point (ZMP) x_z and the ICP x_{icp} can be expressed [9],
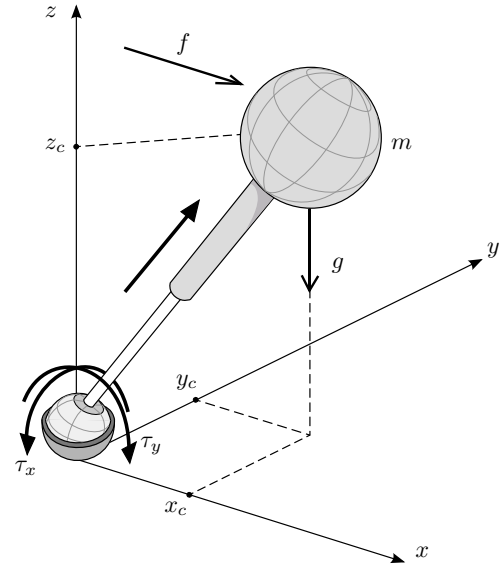

Fig. 2.   The 3D-LIP model used to approximate the dynamics of NAO.

Fig. 3.   Experimental setup used to evaluate the effect of a constant force.

[6] as

$$x_z = x_c - \frac{1}{\omega^2}\ddot{x}_c \qquad x_{icp} = x_c + \frac{1}{\omega}\dot{x}_c \qquad (2)$$

where $(x_c, \dot{x}_c)$ is the state of the LIP. In (1) f_x is a disturbance while τ_y is an input ankle torque. In order to represent NAO's intrinsic posture control, we use τ_y as a control input which stabilizes the state around the origin of the CoM state space, corresponding to the vertical position of the CoM with null velocity. For example using a simple PD, which for the case considered is equivalent to a state feedback,

$$\tau_y = -k_p x_c - k_d \dot{x}_c \qquad (3)$$

the closed-loop system is given by

$$\ddot{x}_c = -\left(\frac{k_p}{mz_c} - \omega^2\right)x_c - \frac{k_d}{mz_c}\dot{x}_c + \frac{f_x}{m}. \qquad (4)$$
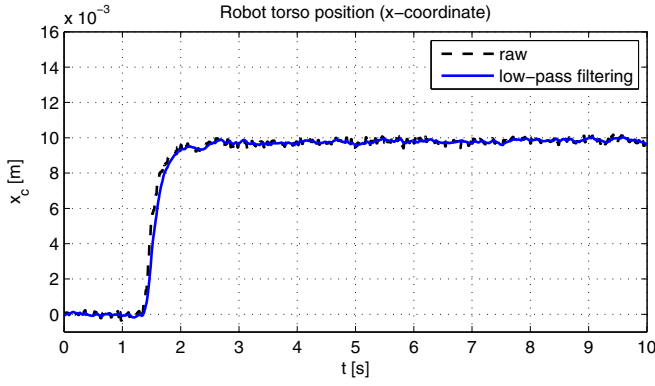
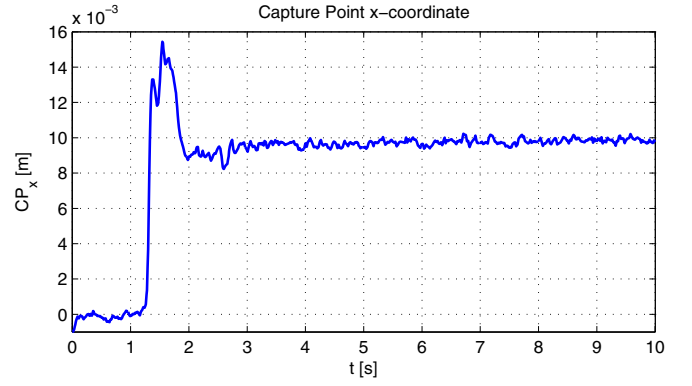Fig. 4. Effect of an external step force on the robot equilibrium: x_c.

Fig. 5. Effect of an external step force on the robot equilibrium: x_{icp}.

This is the humanoid model with a built-in low-level control system. We need to analyze the effect that the force f_x due to the interaction has on the equilibrium of this closed-loop system. The most natural candidate to equilibrium indicator are x_z and x_{icp}. The transfer functions from the interaction force to each of these outputs are:

$$F_z(s) = \frac{x_z(s)}{f_x(s)} = -\frac{s^2 - \omega^2}{m\omega^2[s^2 + sk'_d - (\omega^2 - k'_p)]} \quad (5)$$

$$F_{icp}(s) = \frac{x_{icp}(s)}{f_x(s)} = \frac{s + \omega}{m\omega[s^2 + sk'_d - (\omega^2 - k'_p)]} \quad (6)$$

where $k'_p = k_p/mz_c$ and $k'_d = k_d/mz_c$.

In order to evaluate how well this model matches the real NAO, we performed a step response experiment with respect to the disturbance f_x. The basic experimental setup is shown in Fig. 3: a mass of about 1 Kg has been attached to the robot through a pulley system. With this applied force the robot feet remain in contact with the ground and the adopted interaction model is valid.

The application of this external force perturbs the position of all the three points x_c, x_z and x_{icp} and the system converges to a new forced equilibrium. The measured CoM, ICP and ZMP are shown in Fig. 4, Fig. 5 and Fig. 6 respectively. The torso available measurement data are used as an approximation of the CoM position.

As predicted by the model, at steady-state all three points x_c, x_z and x_{icp} converge to the same constant value. If we consider these outputs as equilibrium indicators, the error on these outputs is the effect that the applied constant force has on the robot equilibrium. This is relevant to the design of the reference walking velocity that will be illustrated in Sect. III.

This fast model validation indicates that system (4) is a reasonable model to determine which of the three points is a good quantity to monitor in order to detect and indirectly measure an external force applied to the robot. Since the CoM always follows the ICP (see eq. (2) or the detailed analysis in [9]), we focus the following discussion on the comparison between the ZMP and ICP responses in order to choose the "best indirect sensor".
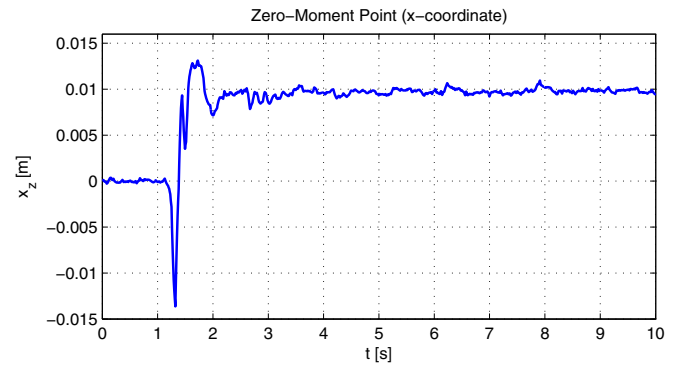

Fig. 6. Effect of an external step force on the robot equilibrium: x_z.

The expressions of the transfer functions (5) and (6) respectively show that they differ in the zeros, that is, in the transient behavior. The main difference lies in the ZMP output having a non-minimum phase characteristic due to the presence of a positive zero in ω. As well-known, in a subsequent control loop, the presence of this positive zero may limit the obtainable closed-loop bandwidth and also have implications in the control effort. Moreover being $F_z(s)$ proper any measurement noise is not filtered. In addition, the step response of the ICP indicates that this output is more sensitive and reacts faster than the CoM to external perturbation and always moves in the direction of the applied force. We thus choose the x_{icp} as the variable available for control. With this choice, $F_{icp}(s)$ can be interpreted as the transfer function of the "built-in" force measurement device.

III. WALKING CONTROL

When a force is applied on the humanoid it generates a perturbation of the robot equilibrium which is well represented by the ICP evolution. The key point in manual guidance is that the force applied by a human is not a force that the humanoid is supposed to contrast but instead it indicates the direction and the intensity of the desired velocity. So, in some sense, the force generates a reference for the biped robot.
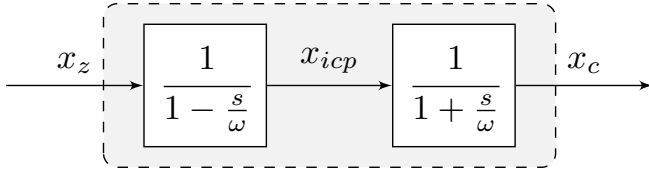
Fig. 7. LIP model representation in (x_{icp}, x_c) coordinates.

Usually the reference for a humanoid is given in terms of a desired ZMP trajectory generated after a sequence of steps has been planned. How to translate the given ZMP trajectory into an equivalent stable CoM is a key problem in motion planning for humanoids since the ZMP to CoM dynamics are unstable. In particular, with the change of coordinates introduced by [8]

$$\begin{pmatrix} x_{icp} \\ x_c \end{pmatrix} = \begin{pmatrix} 1 & 1/\omega \\ 1 & 0 \end{pmatrix} \begin{pmatrix} x_c \\ \dot{x}_c \end{pmatrix} \qquad (7)$$

it is evident that the unstable dynamics is represented by the ICP component as shown in Fig.7 and this is the cause of the difficulties. When a desired ZMP is given, the key point is translating this trajectory into a desired ICP one.

Here we take a different approach. Considering the ZMP as an input and the ZMP to ICP relation in Fig. 7, it easy to verify that the applied force f_x acts as a input disturbance:

$$x_{icp} = \frac{1}{\omega - s}(\omega x_z - \frac{f_x}{m\omega}).$$

Given this model it is in principle possible, using the results in [9], to devise a controller that maintains the system in a desired capturability region by keeping the distance between the ICP and the ZMP within given bounds through walking. The requirement of remaining in a capturability region is to guarantee that the robot will come to rest within a desired number of steps when the applied force becomes null.

This approach is however hard to pursue on the humanoid NAO. First, the robot is poorly reactive due to hardware limitations. Second, while a fast validation of control algorithms is possible using the high level control functions, controlling the robot at low level, as required by the above sketched conceptual scheme, is not easy if not impossible when real-time performance is required.

Therefore, considering our target robotic platform and its high-level control functions, we propose a simple control scheme for the execution of interaction tasks in which the humanoid is expected to walk in the direction of an external force. Given the interaction model of the previous section, when a constant force is applied to the mass the system reaches a new static equilibrium. If the pivot joint of the pendulum is translated with a velocity proportional to the distance of the ICP from its unperturbed equilibrium, the pendulum will move in the direction of the applied force and will stop when the force goes to zero. We will use this intuition in generating a reference velocity for NAO.

A. Reference velocity generation

The reference velocity generated by the equilibrium perturbation due to the applied force is chosen proportional to the relative distance of ICP from its rest position, thus realizing a form of admittance control:

$$\begin{cases} v_x = k_x(x_{icp} - x_{cps}) \\ v_y = k_y(y_{icp} - y_{cps}). \end{cases} \qquad (8)$$

In the above equation k_x and k_y are positive gains, $\boldsymbol{p}_{icp} = (x_{icp}, y_{icp})^T$ is the position of the ICP, $\boldsymbol{p}_{cps} = (x_{cps}, y_{cps})^T$ is the position of the support polygon centroid where the ICP should stay when the robot is at rest and no external force is acting on it. The error $\boldsymbol{p}_{icp} - \boldsymbol{p}_{cps}$ can, in fact, be interpreted as a measure of the applied force.

B. Sway motion cancellation

The reference velocity (8) has been designed considering that the ICP moves under the action of the external force only. However, the ICP position is also perturbed by the walking motion of the humanoid. To isolate the motion of the ICP due to the force it is necessary to filter the transversal oscillation of the torso known as sway motion. In this work we have used the low-pass filter devised in [10] for trajectory control.

IV. EXPERIMENTAL RESULTS

In this section we present the experimental validation of the proposed approach on NAO. The sensory equipment of this humanoid includes an Inertial Measurement Unit (IMU) placed in the torso consisting of a 3-axes accelerometer and two single-axis gyrometers. The accelerometer provides a measurement of the robot *proper* accelerations along the sensor three axes ($\hat{a}_x$, $\hat{a}_y$ and $\hat{a}_z$), the gyrometers measure the rotation velocities around the robot x and y axes (ω_x and ω_y). An on-board filtering algorithm fuses accelerometers and gyrometers data to provide a measure of the robot roll and pitch angles (α and β). The data coming from the IMU have been processed to obtain the robot *effective* acceleration and linear velocities. In particular, to retrive the effective robot acceleration, we first removed the term due to the gravity:

$$a_x = \hat{a}_x - g\sin\beta,$$

$$a_y = \hat{a}_y - g\sin\alpha,$$

where $g = 9.81$ m/s^2, and then we projected them on an inertial frame:

$$\ddot{x}_c = -a_x\cos\beta,$$

$$\ddot{y}_c = -a_y\cos\alpha.$$

Finally, we removed the drift that commonly affect these measures by calibrating the sensor at the beginning of each experiment, and we cleaned the signals with a low-pass frequency filter. Under the assumption that the robot CoM coincides with the origin of the torso frame, $\ddot{x}_c$ and $\ddot{y}_c$ are the measured acceleration used for ZMP computation in the validation of the interaction model in Section II.
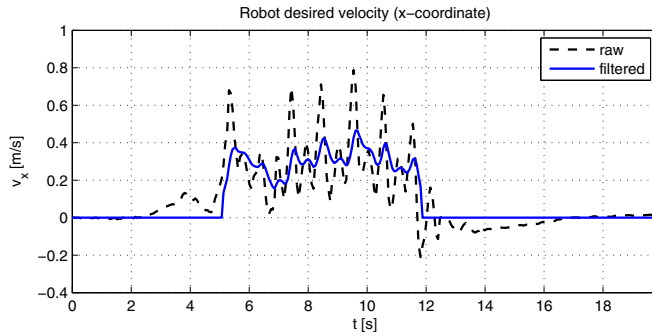
Fig. 8. Constant force experiment: desired velocity along the x-axis.

Fig. 9. Constant force experiment: desired velocity along the y-axis.

The robot CoM velocity in the robot frame is computed by simple trigonometry using gyrometers and orientation information:

$$\dot{x}_c = z_c \ \omega_y \ \cos \beta,$$

$$\dot{y}_c = z_c \ \omega_x \ \cos \alpha.$$

These velocities are used to obtain a measure of the ICP. Also in this case the sensors signals are filtered.

The measures of x_c, y_c and z_c have been obtained using the *getPosition* API method as relative to the NAO frame position which differs from the averaged position of the support polygon centroid by a constant value.

The reference velocity in eq. (8) has been computed using $k_x = 25$ and $k_y = 1$. In these early experiments there has been no fine tuning of these quantities. This velocity has been sent to the robot using the NAO's API method *setWalkTargetVelocity* which allows to set the desired velocity by specifying the incremental step length and stepping frequency, thus providing a natural method to directly control the motion of the polygon of support. This is a "non-blocking" function, i.e., it executes only the last command, thus allowing us to send commands to the robot with an arbitrary frequency. The low-level controller guarantees that when the applied force, and hence the reference velocity, becomes null, the robot takes the necessary number of steps to come to a rest configuration.

A. Application of a constant force

The first experiment is to test the possibility to move the robot with a constant external force. To this end we used the same experimental set-up of Section II. Figure 10 reports six snapshots of the experiment in which NAO successfully walks in the direction of the pulling force generated by the suspended mass. When the mass touches the ground the value of the force becomes zero, the ICP converges to the controlled static equilibrium and the robot stops.

Figure 8 shows the plot of the desired velocity v_x recorded during the experiment. The black-dashed line is the v_x represents the sensor data after a first internal filtering. The blue-solid line reports the result of a second low-pass filtering used to smooth the reference signal. We have also implemented a thresholding operation in order to avoid any excessive chattering in the x direction. In other words the
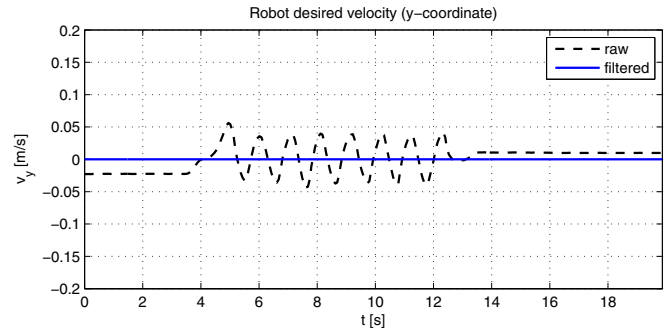
control input will be non zero only if a significant variation in the ICP is detected.

Similarly, Fig. 9 reports the raw and filtered plus thresholded desired velocity in the y direction. The small oscillations of the signal are cancelled by the thresholding operation that is much smaller in this direction and that has been used essentially to filter out numerical chattering.

B. Manual guidance

Finally we have validated the approach with an experiment of human hand-in-hand guidance. Figure 11 shows snapshots of the corresponding video accompanying this paper. The human partner holds NAO by its hands and guides it by applying first a pulling and then a pushing force for some interval of time. NAO correctly reacts by following the motion intention of the human as can be better appreciated in the accompanying video.

V. CONCLUSION

In this paper we present a manual guidance strategy for humanoids that does not require force sensors in the hardware equipment of the robot. The strategy has been designed as a high level control task and is compatible with the humanoid built-in walking controller. The approach has been validated on the robot NAO whose hardware limitations hardly allow to perform complex tasks like physical interaction.

The proposed method relies on an indirect measure of the force generated by the physical interaction with the human based on the perturbation of the equilibrium. An obvious limitation of the method is the inability to distinguish between an intentional (i.e., due to interaction) and an unwanted (due, e.g., to pushes, terrain irregularities, . . .) perturbation of the equilibrium.

Future development of the proposed technique will include force estimation through measures of the joint currents in the spirit of [11] and will investigate the inclusion of vision in the control of interaction. Setting the ideas behind the presented approach in a formal and more general framework is the subject of current study.

REFERENCES

[1] S. Setiawan, J. Yamaguchi, S.-H. Hyon, and A. Takanishi, "Physical interaction between human and a bipedal humanoid robot -realization of human-follow walking," in *1999 IEEE Int. Conf. on Robotics and Automation*, 1999, pp. 361–367.
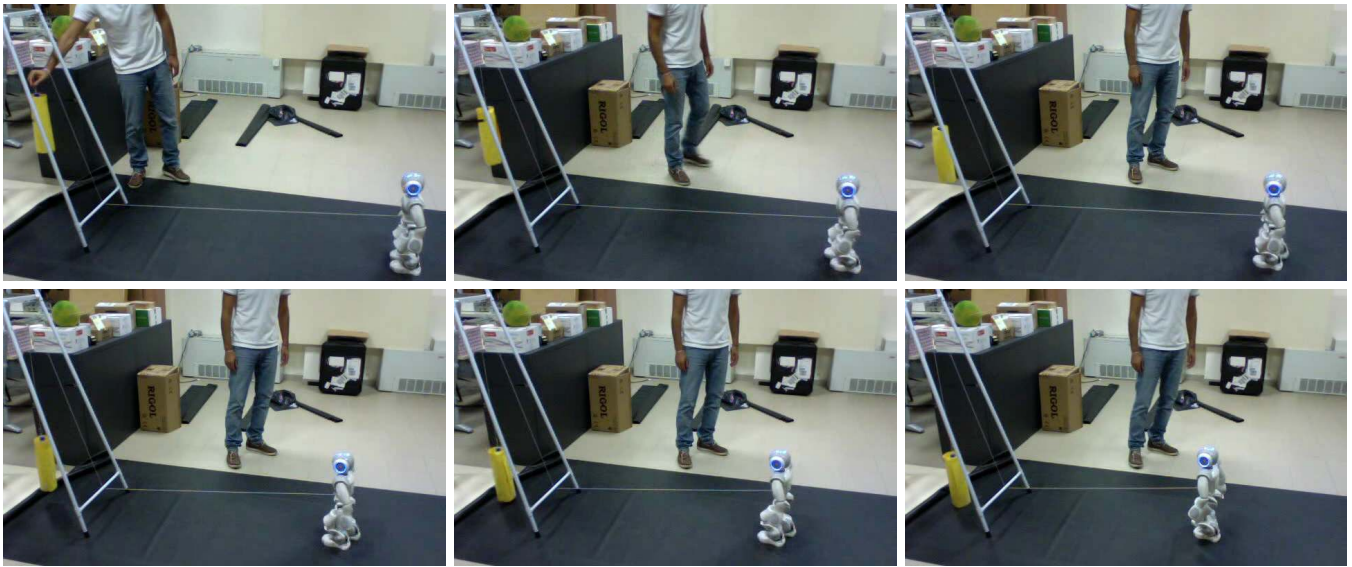
Fig. 10. Application of a constant force: a suspended mass is attached to the torso of NAO through a pulley system. When the mass is released, the robot starts to walk under the action of the force and stops when the mass touches the ground and the applied force goes to zero.
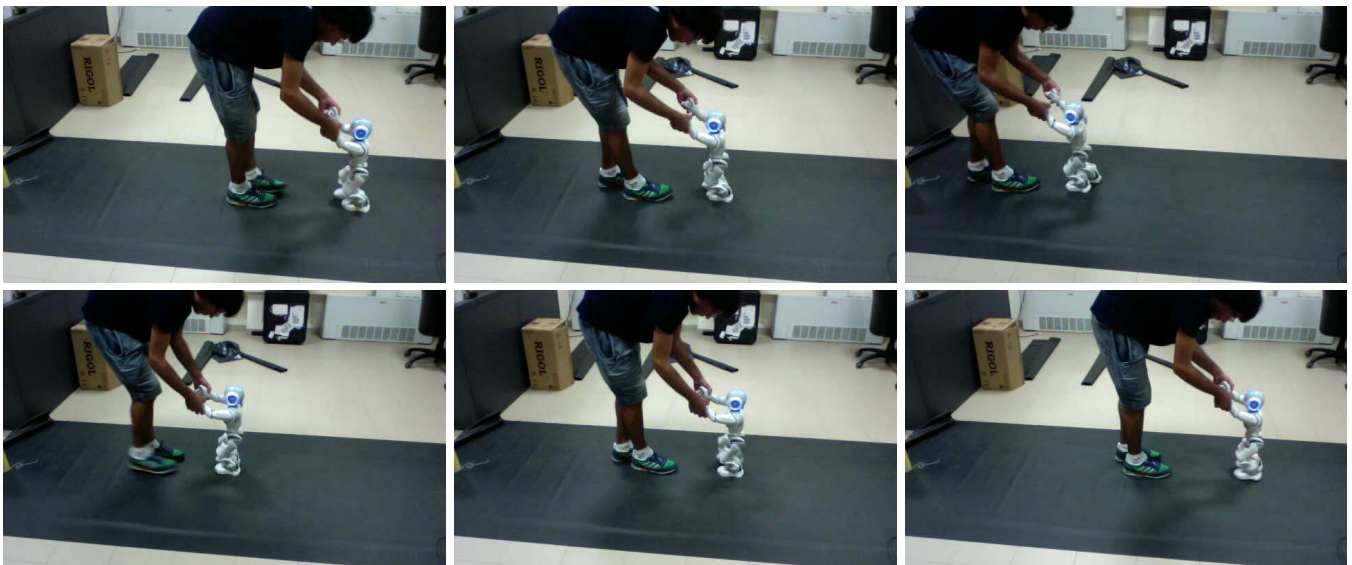

Fig. 11. Manual guidance: NAO is driven by a human partner and walks along the direction of the exchanged force.

[2] K. Yokoyama, H. Handa, T. Isozumi, Y. Fukase, K. Kaneko, F. Kanehiro, Y. Kawai, F. Tomita, and H. Hirukawa, "Cooperative works by a human and a humanoid robot," in *2003 IEEE Int. Conf. on Robotics and Automation*, 2003, pp. 2985–2991.

[3] O. Stasse, P. Evrard, N. Perrin, N. Mansard, and A. Kheddar, "Fast foot prints re-planning and motion generation during walking in physical human-humanoid interaction," in *2009 IEEE-RAS Int. Conf. on Humanoid Robots*, 2009, pp. 284–289.

[4] A. Bussy, A. Kheddar, A. Crosnier, and F. Keith, "Human-humanoid haptic joint object transportation case study," in *2012 IEEE/RSJ Int. Conf. on Intelligent Robots and Systems*, 2012, pp. 3633–3638.

[5] P.-Y. Oudeyer, O. Ly, and P. Rouanet, "Exploring robust, intuitive and emergent physical human-robot interaction with the humanoid robot Acroban," in *2011 IEEE-RAS Int. Conf. on Humanoid Robots*, 2011, pp. 120–127.

[6] J. Pratt, J. Carff, S. Drakunov, and A. Goswami, "Capture point: A step toward humanoid push recovery," in *2006 IEEE-RAS Int. Conf. on Humanoid Robots*, 2006, pp. 200–207.

[7] A. L. Hof, "The 'extrapolated center of mass' concept suggests a simple control of balance in walking," *Human Movement Science*, vol. 27, pp. 112–125, 2008.

[8] J. Englsberger, C. Ott, M. A. Roa, A. Albu-Schäffer, and G. Hirzinger, "Bipedal walking control based on capture point dynamics," in *2011 IEEE/RSJ Int. Conf. on Intelligent Robots and Systems*, 2011, pp. 4420–4427.

[9] T. Koolen, T. D. Boer, J. Rebula, A. Goswami, and J. E. Pratt, "Capturability-based analysis and control of legged locomotion. part 1: Theory and application to three simple gait models," *The International Journal of Robotics Research*, vol. 31, no. 9, pp. 1094–1113, 2012.

[10] G. Oriolo, A. Paolillo, L. Rosa, and M. Vendittelli, "Vision-based trajectory control for humanoid navigation," in *2013 IEEE-RAS Int. Conf. on Humanoid Robots*, 2013, pp. 118–123.

[11] M. Geravand, F. Flacco, and A. De Luca, "Human-robot physical interaction and collaboration using an industrial robot with a closed control architecture," in *2013 IEEE Int. Conf. on Robotics and Automation*, 2013, pp. 4000–4007.